Magnetic blanketing in white dwarfs

D. T. Wickramasinghe and Brian Martin* *Department of Mathematics, Faculty of Science, Australian National University, GPO Box 4, Canberra, ACT 2601, Australia*

Summary. The influence of a strong magnetic field on line blanketing in white dwarfs is studied using a modified version of the model atmosphere programme Atlas. The splitting of the hydrogen lines is incorporated into the programme using an accurate but simple solution for the intensity in the polarized radiative transfer equations. When line broadening is assumed unchanged, magnetic line blanketing removes about 10 per cent more flux at 50 or 100 MG than at zero field; when the line components in a magnetic field are assumed to be only Doppler broadened, total line blanketing is greatly reduced. The magnetic line-blanketed atmosphere is not sufficiently different from the zero-field atmosphere to greatly affect previous line models of magnetic white dwarfs, since in most cases magnetic broadening (broadening caused by field spread) is the most important determinant of the appearance of the spectrum in the optical region.

1 Introduction

Over a dozen white dwarfs have been observed which show evidence of large magnetic fields, over 1 MG (Angel 1978; Angel, Borra & Landstreet 1981). The observations show either shifts and splitting in the absorption lines due to the Zeeman effect, or significant values of polarization, or both.

Considerable theoretical work has gone into modelling particular magnetic white dwarfs, and in modelling the general effects of a magnetic field. A model involves the following factors, among others:

(i) Atmospheric structure. Until now, the atmospheric structure has been assumed to be unaffected by the magnetic field. Some of the early calculations assumed a Unno atmosphere, namely with the source function B linear in optical depth τ (Borra 1976; Liebert, Angel & Landstreet 1975). Others have used 'realistic' zero-field model atmospheres (Wickramasinghe & Martin 1979; O'Donoghue 1980).

*Present address: Department of History and Philosophy of Science, University of Wollongong, PO Box 1144, Wollongong, NSW 2500, Australia

(ii) *Magnetic field distribution.* The standard assumption here is a dipole field uniform in optical depth, without anomalies or hotspots. Sometimes the dipole field is offset from the centre of the star, or a quadrupole component introduced (see Martin & Wickramasinghe 1984). An alternative method, adopted for computational convenience more than physical reality, is a field whose magnitude fits a Gaussian distribution (Greenstein, Henry & O'Connell 1985).

(iii) *Continuum absorption.* The continuum is assumed to be polarized following the prescription of Lamb & Sutherland (1974). Their calculations break down at high fields (>50MG roughly), but no high-field calculation is yet available.

(iv) *Line opacities.* These are assumed to be shifted as a function of the magnetic field strength. Tables of shifts have been provided by different authors, including Smith *et al.* (1972), Kemic (1974), Forster *et al.* (1984) and Henry & O'Connell (1985). The recent calculations by Forster *et al.* and by Henry & O'Connell have opened up the possibility of modelling very-high-field magnetic white dwarfs (>100MG), although the lack of calculations about continuum shifts remains a major obstacle.

(v) *Magneto-optical effects.* The magneto-optical parameters cause the plane of polarization to rotate. The parameters associated with the lines do not have a major impact on solutions to the radiative-transfer equations (Martin & Wickramasinghe 1981) but those associated with the continuum do (Martin & Wickramasinghe 1982). Expressions for these parameters in the continuum are given by Pacholczyk (1976).

(vi) *Polarized radiative transfer.* A number of methods have been used, including the Unno solution (Unno 1956), Runge–Kutta methods (Beckers 1969), a perturbation solution based on normal modes (Hardorp, Shore & Wittmann 1976) and a stepwise Unno solution (Martin & Wickramasinghe 1979). These methods vary in their accuracy, convenience and computation time (see Martin & Wickramasinghe 1979).

Our purpose in this paper is to report the results of an effort to test the main assumption involved in the first of these points: the assumption that the magnetic field does not affect the structure of the atmosphere. By including the effect of the magnetic field on the atmospheric structure via blanketing, we aim to remove one more of the limitations to models of magnetic white dwarfs.

2 The model

We started with ATLAS, the computer program widely used to generate atmospheric structures (Kurucz 1971). Our aim was to modify this program to include the effect of the magnetic field on line blanketing.

The first change made in ATLAS was to suppress convection. In a large magnetic field, normal convective processes are inhibited, primarily through the resistance to large-scale motions provided by the magnetic flux lines.

We did not at this stage make any changes in the atmospheric structure equations to incorporate the effect of the magnetic field on energy and pressure equations. An evaluation of the possible effects has been carried out by Landstreet (1985).

The most obvious effect of the field is to split the continuum and line absorption. Rather than a single absorption coefficient η, there now become three components for absorption, indicated by η_p, η_r and η_l. When there is no field, $\eta_p = \eta_r = \eta_l = \eta$, and the polarized radiative-transfer equations reduce to the unpolarized case, as shown in the next section. The problem here is to determine the values η_p, η_r and η_l in the lines and the continuum.

At this stage we have modelled only hydrogen atmospheres. The lines which concern us are the Lyman and Balmer lines. For Lyman lines we used the tabulated shifts and strengths provided by

Smith *et al.* (1972). They give results only for Lyα and Lyβ, but this is quite sufficient since due to the high opacity of these lines the higher Lyman lines have little additional effect on the flux.

For the Balmer lines we used the tabulated shifts and strengths provided by Kemic (1974). An extra multiplicative factor of 3 must be included in Kemic's formula for the oscillator strengths f_{ij} (see Appendix). The Balmer lines – especially Hα and Hβ – are the important lines for blanketing purposes at the atmospheric temperatures which concern us. Kemic tabulates shifts and strengths for Hα to 100 MG, Hβ to 50 MG, Hγ to 20 MG, Hδ to 10 MG and no values for Hε and above. Above the highest listed field strength in Kemic's tables we simply leave the component at the wavelength and strength for the highest tabulated field strength. This seems preferable to extrapolation, which often unphysically leads to wavelengths blueward of the Balmer jump. For Hε and above we use no shifts at all, simply reverting to the ATLAS calculation.

The inaccuracies in line-component shifts do not matter very much, since what counts is that a set of components split and thus absorb at more different wavelengths than at zero-field. At high fields of 50–100 MG, Hγ and above in particular are shifted blueward, congregating just redward of the Balmer jump (which itself is split by the magnetic field). The very approximate procedure adopted here reproduces the congregation of components in this fashion quite well.

A key uncertainty in the calculation is the width of the line components in the presence of a magnetic field. There are no calculations to tell just how wide they will be.

For the zero-field case, we replaced the ATLAS line profiles for Lyα, Lyβ and Hα to Hδ by Voigt profiles. This is because we need to be able to obtain the strength of many components at different places in their profiles quickly and conveniently. The Voigt profile also allows the incorporation of magneto-optical effects in the lines if desired. We adjusted the width of the Voigt profile to mimic the standard ATLAS Stark broadened Lyman and Balmer lines. Rather than the usual width of $3F_0 k_{nm}$ (Kurucz 1971) – which resulted in lines which were much too broad – we found that $F_0 k_{nm}/4$ for Lyman and $F_0 k_{nm}$ for Balmer lines gave good fits. The zero-field flux for a pure hydrogen white dwarf atmosphere with effective temperature $T_e = 12\,000$ K and gravity log $g = 8.0$ is shown in Fig. 1, for comparison with later models.

To determine the effect of different values of the linewidths in the presence of a magnetic field,
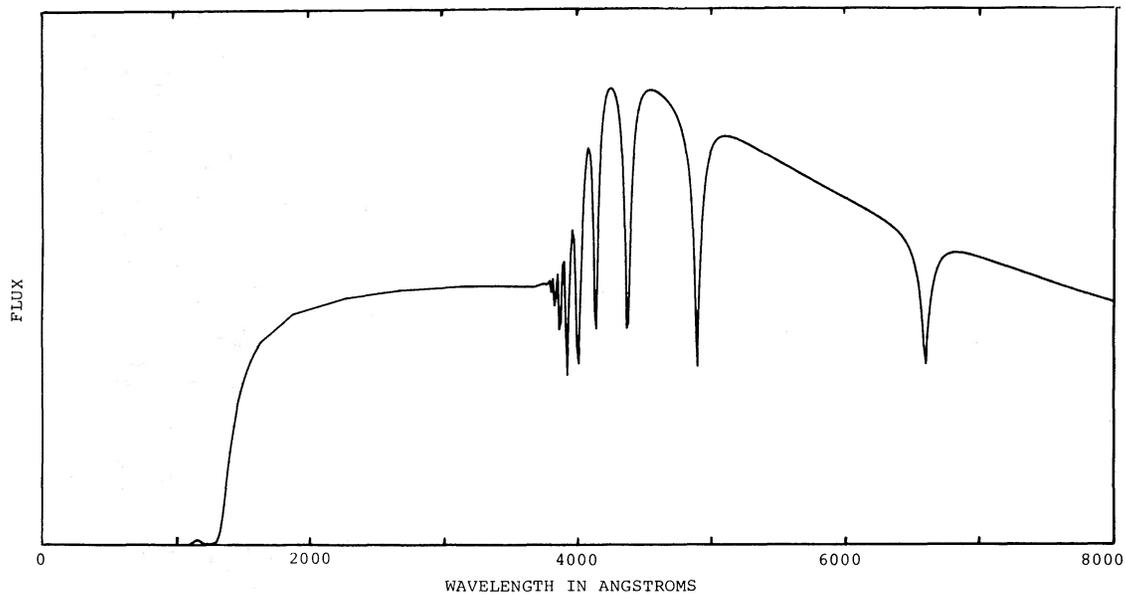
Figure 1. The zero-field flux F_ν from a pure hydrogen white dwarf atmosphere with effective temperature $T_e = 12\,000$ K and gravity log $g = 8.0$, with Voigt line profiles whose widths are adjusted to replicate the usual ATLAS profiles. At the top of the graph $F_\nu = 0.001$ erg cm^{-2} s^{-1} Hz^{-1}.

we used two assumptions which give an upper and lower bound for the blanketing effect. The first assumption is that each of the split components has the same width as at zero-field. This maximizes magnetic blanketing. The second assumption is that the split components are Doppler broadened only. This minimizes blanketing. (In practice, since the Doppler widths are so narrow, we used an ATLAS model with *no* lines to produce a lower bound for magnetic blanketing.) The results show that calculations of line broadening in the presence of a magnetic field are crucial if more accurate determination of magnetic blanketing is to be made.

3 Radiative transfer

In full generality, polarized radiative transfer is a very complex problem. To implement a solution without some sort of simplification would require inordinate computing effort. Therefore we have made several simplifying assumptions and approximations to bring the problem under control.

The first assumption involves scattering. In the presence of a magnetic field, the scattering of a beam of radiation depends on the polarization of the beam (Stenflo 1971). Here we assume that polarized radiation scatters exactly like unpolarized radiation. Therefore we can simply use the existing routines for scattering cross-sections and for iterative solution of the radiative-transfer equations which already exist in the ATLAS program. It turns out that at the effective temperature and gravities that we consider, scattering is not the major effect we are concerned with, so this assumption has only a small effect on our results.

Even without scattering, the radiative-transfer equations for polarized light are formidable. They can be written as follows in terms of the four Stokes parameters I, Q, U and V (Hardorp *et al.* 1976):

$$\mu \frac{dI}{d\tau} = \eta_I(I-B) + \eta_Q Q + \eta_V V, \tag{1}$$

$$\mu \frac{dQ}{d\tau} = \eta_Q(I-B) + \eta_I Q - \varrho_R U, \tag{2}$$

$$\mu \frac{dU}{d\tau} = \varrho_R Q + \eta_I U - \varrho_W V, \tag{3}$$

$$\mu \frac{dV}{d\tau} = \eta_V(I-B) + \varrho_W U + \eta_I V. \tag{4}$$

Here τ is the optical depth, $\mu = \cos\theta$ where θ is the angle between the direction of propagation and the axis along which τ is measured, and B is the local source function. The absorption parameters η_I, η_Q and η_V are given by:

$$\eta_I = \tfrac{1}{2}\eta_p \sin^2\xi + \tfrac{1}{4}(\eta_l + \eta_r)(1 + \cos^2\xi), \tag{5}$$

$$\eta_Q = [\tfrac{1}{2}\eta_p - \tfrac{1}{4}(\eta_l + \eta_r)] \sin^2\xi, \tag{6}$$

$$\eta_V = \tfrac{1}{2}(\eta_r - \eta_l) \cos\xi. \tag{7}$$

ξ is the angle between the direction of propagation and the direction of the local magnetic field. η_p, η_l and η_r are the ratios of the respective sums of the total absorption coefficients of the three shifted Zeeman components and the shifted continuum absorption coefficients to the unshifted continuum absorption coefficient. ϱ_R and ϱ_W are the magneto-optical parameters. In Hardorp *et*

al.'s (1976) formulation (1)–(4), the solution pair (Q/U) must be multiplied by

$$\begin{bmatrix} \cos2\ \phi & -\sin2\ \phi \\ \sin2\ \phi & \cos2\ \phi \end{bmatrix}. \tag{8}$$

The angle ϕ is the azimuth with respect to an arbitrary x-axis at right angles to the line-of-sight.

To implement a solution to (1)–(8) in ATLAS would be an enormous task, to be undertaken only if the effects were significant and simpler methods were inadequate. There are various approximate solutions available which have advantages and disadvantages in different circumstances (Martin & Wickramasinghe 1979). All, however, involve either a substantial increase in computational effort or serious inaccuracies in some circumstances. For our present purposes we only require an accurate solution for the intensity I. The values of Q, U and V which give linear and circular polarization are not of interest. For this situation we have developed a very simple solution which is surprisingly accurate in most relevant circumstances. Since this solution may be of use for other purposes, we describe it here in some detail.

We call this solution the one-component approximation, because it is based on a solution to the unpolarized radiative-transfer equation for I, which can be interpreted as one component of the four-component solution for I, Q, U and V.

First we present a solution method for the unpolarized transfer equation, which can be written in the no-scattering case as

$$\mu\ \frac{dI}{d\tau} = \eta(I-B). \tag{9}$$

We assume that the source function B and the opacity η are given at a series of optical depths $\tau_0 = 0, \tau_1, \tau_2, \ldots, \tau_N$. We assume we know the solution at depth τ_n, and wish to derive the solution at the adjacent depth nearer the surface, τ_m. We assume that in the region (τ_m, τ_n) that the intensity I varies as follows:

$$I = I_a + I_b(\tau - \tau_m) + I_c \exp\left[d(\tau - \tau_m)\right]. \tag{10}$$

We also assume that the source function is linear in the region (τ_m, τ_n):

$$B = B_m[1 + \beta(\tau - \tau_m)], \tag{11}$$

where B_m is the value of B at τ_m.

Substituting (10) and (11) into (9) and setting constant terms equal to each other and likewise for terms multiplying τ and $\exp[d(\tau - \tau_m)]$, we obtain

$$I_m = B_m(1 + \mu\beta/\eta) + \{I_n - [B_m(1 + \mu\beta/\eta) + B_m\beta\ \Delta\tau]\}\ \exp\left(-\eta\ \Delta\tau/\mu\right) \tag{12}$$

where $\Delta\tau = \tau_n - \tau_m$. If we start at τ_N with the solution

$$I_N = B_N(1 + \mu\beta/\eta) \tag{13}$$

then repeated applications of (12) will give the solution at $\tau_0 = 0$. In general η as well as β will vary with τ.

Looking at the solution (12), we see that it is based on the local solution $I = B(1 + \mu\beta/\eta)$ which applies in a Unno atmosphere [namely an atmosphere with $B = B_0(1 + \beta\tau)$], perturbed by the previous solution I_n to the extent that I_n is different from the Unno solution at τ_n. This suggests that we may be able to modify (12) to apply to the polarized radiation case by looking at the Unno solution to the full set of equations (1)–(4). The solution for I in a Unno atmosphere with $B = B_0(1 + \beta\tau)$ can be written:

$$I = B_0(1 + \beta\mu\eta_I/D), \tag{14}$$

$$D=\eta_I^2-\left(1-\frac{\varrho_R^2}{\eta_I^2+\varrho_R^2+\varrho_W^2}\right)\eta_{QU}^2-\frac{2\varrho_R\varrho_W\eta_{QU}\eta_V}{\eta_I^2+\varrho_R^2+\varrho_W^2}-\left(1-\frac{\varrho_W^2}{\eta_I^2+\varrho_R^2+\varrho_W^2}\right)\eta_V^2, \tag{15}$$

where $\eta_{QU}=\sqrt{\eta_Q^2+\eta_U^2}$.

This solution is analogous to the unpolarized Unno solution, except that η is replaced by D/η_I.

With these expressions, our one-component solution for I is quite simple: we solve for I using (12), except that in each stage we replace η by D/η_I.

Tables 1 and 2 give results indicating the accuracy of the one-component solution. In Table 1 we present results for the case with a realistic temperature structure but constant opacities and magneto-optical parameters. The accuracy is good in most circumstances. When there are no

Table 1. Exact and one-component solutions for the intensity in an atmosphere with constant opacities and magneto-optical parameters. (The seemingly arbitrary continuum parameter values of $\eta_p=1.00$, $\eta_l=0.66$, $\eta_r=1.54$, $\varrho_R=771$, $\varrho_W=68$ are actually the values at 5200 Å, $\tau=1$.) The temperature structure is taken from a zero-field, log $g=8.0$ white dwarf atmosphere with $T_e=12\,000$ K (Wickramasinghe 1972). The 'exact' intensities I_e are calculated using the method of Martin & Wickramsinghe (1979) with the full set of polarized radiative-transfer equations. The one-component solution I_1 is given by (14) and (15).

η_p	η_l	η_r	ϱ_R	ϱ_W	I_e	I_1
1.00	0.66	1.54	0	0	2.6452	2.6459
100	0.66	1.54	0	0	1.8850	2.0719
1.00	100	1.54	0	0	1.8494	2.0360
1.00	100	100	0	0	1.1084	1.1100
100	100	1.54	0	0	1.1394	1.1456
1.00	0.66	1.54	771	68	2.6447	2.6453
100	0.66	1.54	771	68	1.2160	1.2202
1.00	100	1.54	771	68	1.7550	1.9066
1.00	100	100	771	68	1.1034	1.1037
100	100	1.54	771	68	1.1234	1.1259

Table 2. Exact and one-component solutions for the intensity in an atmosphere with realistic opacities and magneto-optical parameters. The atmospheric structure is taken from a zero-field, log $g=8.0$ white dwarf atmosphere with $T_e=12\,000$ K (Wickramasinghe 1972). The magneto-optical parameters in the continuum are taken from Pacholczyk (1976); these are large at all optical depths. No magneto-optical parameters associated with the lines are incorporated since they are much smaller (Martin & Wickramsinghe 1981). The 'exact' intensities I_e and circular polarizations V_e are calculated using the method of Martin & Wickramsinghe (1979) with the full set of polarized radiative-transfer equations. The one-component solutions for I_1 and V_1 are given by (14)–(16). Intensities have been multiplied by 1000, and the circular polarizations are given in per cent.

λ, Å	Type of absorption	I_e	I_1	V_e	V_1
4000	continuum only	0.4176	0.4193	−9.12	−13.32
6840	continuum only	0.2226	0.2237	−7.32	−13.38
6470	strong p-component	0.1208	0.1208	−0.026	−0.026
6143.5	weak p-component	0.1290	0.1290	−0.62	−0.61
7368.4	strong l-component	0.1202	0.1202	4.04	4.02
7412.9	weak l-component	0.1363	0.1374	15.11	15.82
5411.4	strong r-component	0.1217	0.1216	−0.93	−0.88
5805.2	weak r-component	0.1305	0.1303	−6.12	−5.97
6480	p-component wing	0.1502	0.1502	−1.24	−2.84
6490	p-component wing	0.1711	0.1713	−2.11	−5.74
7420	l-component wing	0.1702	0.1747	16.15	20.27
7430	l-component wing	0.1824	0.1838	10.76	8.72
7400	r-component wing	0.1755	0.1786	14.14	15.53
7390	r-component wing	0.1740	0.1776	14.74	16.95

magneto-optical effects, the accuracy is very high except in the case of an isolated component, and even in this case the result is only about 10 per cent off. When there are large magneto-optical parameters, the accuracy is very high except in the case of an isolated *l* or *r* component.

The results in Table 1 are only for a realistic temperature structure. For other temperature structures, the following applies. For a Unno atmosphere, the one-component method gives exact results, as indeed its derivation demands. When the temperature gradient is steeper than the Unno atmosphere in which *B* is linear in τ – for example $B=1+\tau^{3/2}$ – the one-component solution underestimates the solution, producing excess absorption. When the temperature gradient is shallower than the Unno atmosphere – for example $B=1+\tau^{1/2}$ – the one-component solution overestimates the solution, producing insufficient absorption. This is what the realistic temperature distribution used for Table 1 does. Clearly, the closer the temperature distribution to the Unno form, the more accurate the one-component solution. A grey atmosphere gives much more accurate results than shown in Table 1.

Table 2 gives results for a situation typical of a real atmosphere. There is a variation of opacities and magneto-optical parameters as well as temperature with optical depth, taken from a $T_e=12\,000$ K model atmosphere. The results show that the one-component solution for *I* is quite accurate for parameter variations typical of a magnetic white dwarf.

The success of the one-component solution for *I* is so encouraging that it is worth looking at the analogous solutions for *Q*, *U* and *V*. Following the same procedure as before, which means setting $Q_n=U_n=V_n=0$ for $n>0$ when solving for I_m, we find that Q_m, U_m and V_m depend only on I_m and the other parameters at τ_m. By looking at the relation betwen the Unno solutions for *I*, *Q*, *U* and *V*, simple expressions for *Q*, *U* and *V* in terms of the one-component solution for *I* can be found. For example,

$$V_1=-\left(\frac{1+[\varrho_R\varrho_W/(\eta_I^2+\varrho_R^2)]\eta_{QU}/\eta_V}{1+\varrho_W^2/(\eta_I^2+\varrho_R^2)}\right)B_0\beta\mu\eta_V/D. \tag{16}$$

Unfortunately, the one-component method does not give very accurate results for *Q*, *U* or *V*. Results for *V* are shown in Tables 1 and 2 to illustrate this. Usually the result for *V* is correct within a factor of 2, but that is all.

Why does the one-component method work so well for *I* but not for the other Stokes parameters? One way to understand this is in terms of the size of *I*, *Q*, *U* and *V*. In most circumstances *Q*, *U* and *V* are much smaller than *I*. The one-component solution leaves out the effect of *Q*, *U* and *V* on *I*, while including the effect of η_Q, η_U, η_V, ϱ_R and ϱ_W as well as η_I on *I* via the term D/η_I. Since *Q*, *U* and *V* are to a considerable extent determined by the local values of B, η_I, η_Q, η_U, η_V, ϱ_R and ϱ_W, the one-component solution for *I* takes into account much of the contribution from *Q*, *U* and *V* in the original equations. By contrast, *Q*, *U* and *V*, being smaller, are much more sensitive to deviations from a Unno atmosphere. A small inaccuracy in *I* therefore normally will correspond to a much larger inaccuracy in *Q*, *U* and *V*.

For the purposes of altering ATLAS to include magnetic blanketing, we simply replace the opacity η in the program by the one-component value D/η_I. Scattering is included when computing the source function following the usual procedure in ATLAS. The results in Tables 1 and 2 show that the resulting intensity will be more than accurate enough for the purposes of the program.

It should be noted that in the limit of small magnetic field, the expression D/η_I reduces to η because in this limit $\eta_p=\eta_r=\eta_l=\eta$.

We tried out one other approximate solution using one component, namely replacing η by $(\eta_p+\eta_r+\eta_l)/3$. This substitution also provides the correct limit for small magnetic field. However, it gives grossly inaccurate results: in particular, the split components of the lines become far too deep.

4 Flux removal

Before moving to the results, it is worth examining the impact of magnetic line blanketing in a more idealized context to provide some insight into the possible effects in real atmospheres. Consider a single isolated absorption line in the absence of a magnetic field. It removes some amount of flux from the spectrum. Now imagine that the line is split by a magnetic field into n different components of equal strength which are entirely separated from each other. In practice the components would overlap, but by assuming that they are entirely separated we obtain a maximum estimate of the flux removed (compared to the spectrum in the presence of the magnetic field with no lines). Because each of the n components has only $3/n$ the strength of the original line – the factor of 3 is due to the fact that the absorption coefficient for each of the three components p, l and r equals the unshifted absorption coefficient – any single component will not remove as much flux as the line. But if the line is so strong that the core is saturated and the core absorption removes most of the flux, then – so it might seem – the flux removed by the core of any one of the n components would approach the flux removed by the core of the line. This is indeed the case under one condition: that there is mixing between the two normal modes of propagation of the polarized radiation. This will occur if substantial magneto-optical effects are present. However, when the magneto-optical parameters are equal to zero there will be no mixing between the two modes and the flux removed from the core of any component can be at most one-half the flux removed from the core of the line.

Our calculations show that this expectation is borne out. In the centre of a deep and narrow line, the flux removed by n completely separated components each with strength $3/n$ of the line strength approaches n times the flux removed by the single line. But this result applies only in the core. In the wings the ratio is much less, and in the far wing the n components remove exactly the same amount of flux as the line. When the flux removed is integrated over the entire line profile, the ratio of flux removed by components to the flux removed by the line can vary between n and 1 depending on how deep and narrow the line is.

We have made one other important assumption in this account: the linewidth of the components is exactly the same as the width of the original line. In practice, the magnetic field will cause a reduction in the width of the components, but theory is not sufficient to tell us what the reduction is. So the calculation here gives an upper limit for the increase in flux removed.

Table 3. The ratio of flux removed from the continuum by n completely separated components of a line to the flux removed by the line itself from the continuum, for a number of cases. The atmospheric structure is the zero-field, $\log g=8.0$, $T_e=12\,000$ K model atmosphere taken from Wickramasinghe (1972). The zero-field flux removed is calculated using $\mu=0.8$, $\eta=1.00$ (continuum opacity) and $\eta_0=100$ (line strength). For calculating the flux removed in the case of separated components, the 'standard' case has the following constant parameters: $n=15$, $\mu=0.8$, $\cos\xi=0.7$, $\eta_p=1.00$, $\eta_l=1.66$, $\eta_r=1.54$, $\varrho_R=771$, $\varrho_W=68$, $a=10$ where a is the linewidth divided by $\Delta\lambda_D$. Only the parameters which are altered from this 'standard' set are listed below.

Parameters	Ratio
'standard'	1.90
$\eta_0=10\,000$	3.34
$\eta_0=1$	1.06
$n=27$	2.05
$\varrho_R=\varrho_W=0$	1.85
$a=0.1$	4.43
$\eta_p=2.00$, $\eta_l=1.19$, $\eta_r=3.37$, $\varrho_R=1397$, $\varrho_W=163$	1.71

Table 3 shows the ratio of the flux removed by a set of components to the flux removed by the line for a standard case and for a number of variants. We note that when the line strength is increased, the ratio increases, as expected. When the line is very weak, there is hardly any increase in flux removed in the presence of a magnetic field. More components increases the flux removal, but not by all that much. Setting the magneto-optical parameters equal to zero does not have much impact at all: the flux removal in the core is reduced by a factor of 2, but the flux removal in the core is only a small portion of the overall flux removal. A narrower line increases the flux removal, as expected. A stronger continuum reduces the flux removal, because the depth of the line is not as great in this case.

What can be concluded from these results? First, magnetic blanketing does not increase the flux removed from the continuum by as much as might have been expected: a factor of 2 or 3 is perhaps the most that can be expected, and this would only apply in the ideal case in which the components are entirely separated. Second, if the linewidths of the shifted components are less than the original line, then there may actually be less blanketing than in the original spectrum. Finally, a glance at Fig. 1 shows that even doubling or tripling the flux removed by the Balmer lines (the Lyman lines do not shift enough to have a major effect) would not be all that dramatic. We conclude that magnetic blanketing may not live up to its promise of being a major effect – except possibly in the negative sense of *reducing* line blanketing.

5 Results

We have computed a series of pure hydrogen white dwarf atmospheres for an effective temperature $T_e = 12\,000$ K and gravity log $g = 8.0$ using our modified version of ATLAS. Convection has been suppressed in all calculations. Line-blanketed flux spectra at a magnetic field $B = 50\,\mathrm{MG}$, in which the field is always at an angle of $45°$ with respect to the normal to the surface, are shown in Figs 2–5 for various assumptions about the line spectra. When broadening is assumed unchanged by the field (Fig. 2), line blanketing removes 8–14 per cent more flux at $50\,\mathrm{MG}$ than at zero-field.
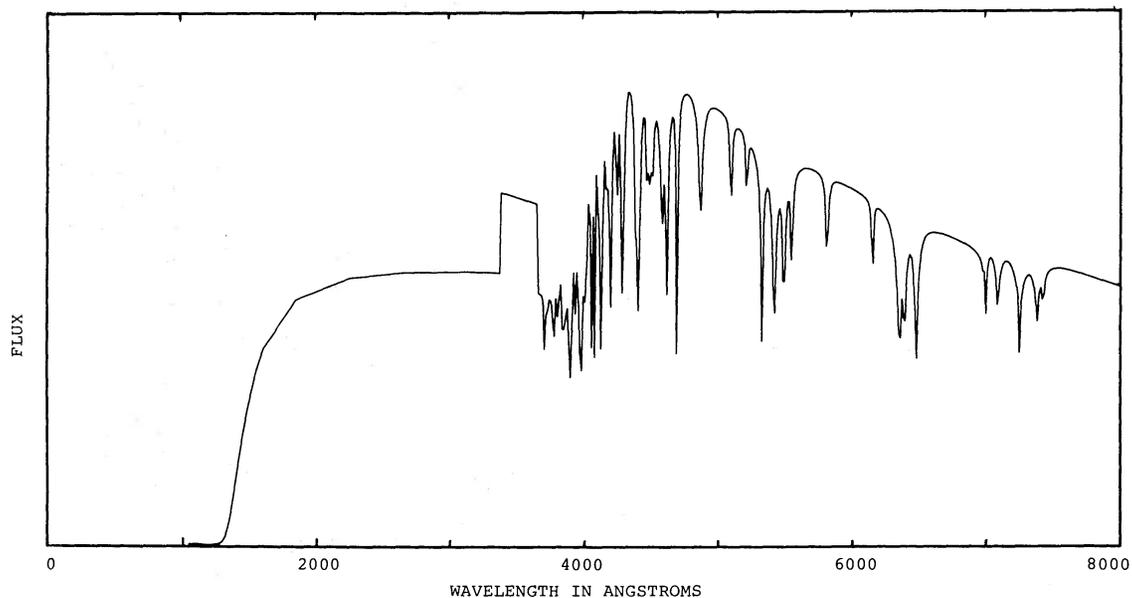
Figure 2. Flux F_v from a pure hydrogen white dwarf atmosphere with effective temperature $T_e = 12\,000$ K and gravity log $g = 8.0$, in the presence of a uniform magnetic field of strength $B = 50\mathrm{MG}$ orientated everywhere at an angle $45°$ with respect to the normal to the surface. The widths of the Voigt profiles are the same as for the zero-field case. Other assumptions and approximations are described in the text. At the top of the graph $F_v = 0.001$ erg cm^{-2} s^{-1} Hz^{-1}.
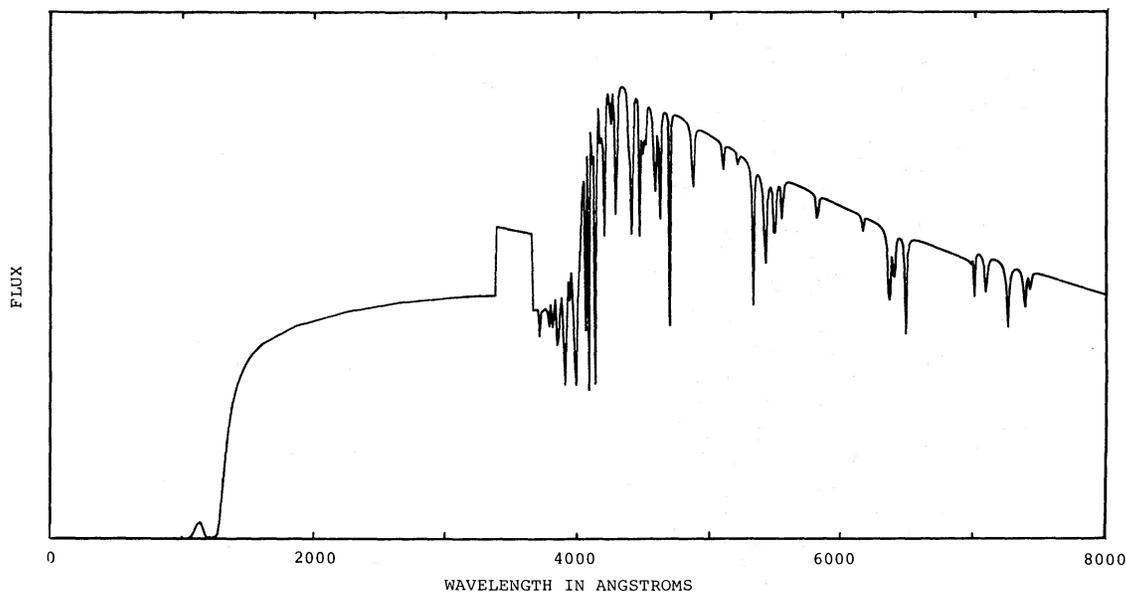
Figure 3. As Fig. 2, except that linewidths are reduced by a factor of 10. Note that the shifted Paschen jump can be seen just blueward of 7000 Å.
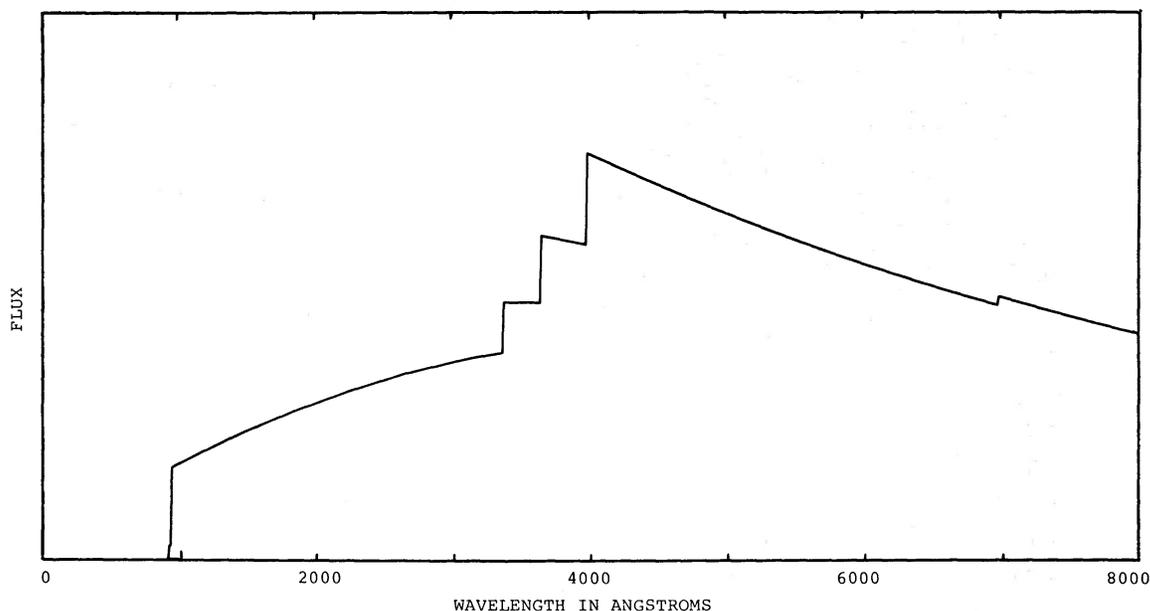
Figure 4. As Fig. 2, except that there are no lines. The atmosphere approximates the case with Doppler broadening only.

When line components are reduced to 0.1 of the zero-field width (Fig. 3), 8–12 per cent less flux is removed. If there are no lines – approximating the case in which the lines are only Doppler broadened – (Fig. 4), 60–90 per cent less flux is removed. Finally, Fig. 5 shows the importance of including continuum magneto-optical effects.

The change in the degree of line blanketing has associated effects on the temperature and pressure structure of the atmosphere which in turn affects the appearance of the continuum and of the spectral lines. These effects are well known from the theory of stellar atmospheres and will not be discussed here. It should be noted that the major differences in the appearance of the spectral
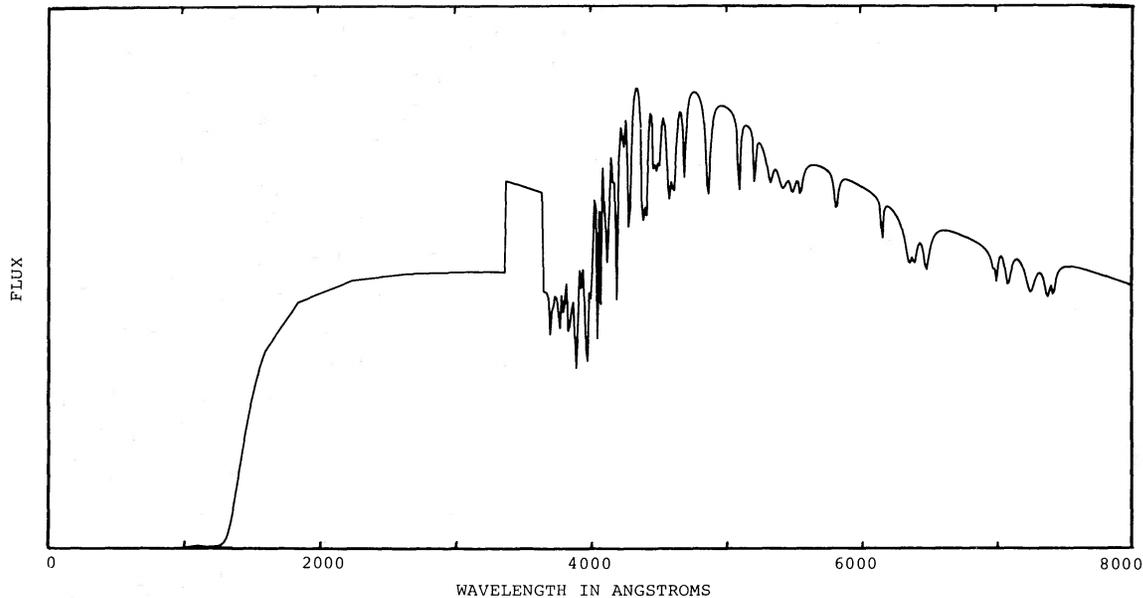
Figure 5. As Fig. 2, except that there are no magneto-optical effects.

lines in Figs 2–5 are caused by changes in the linewidth and magneto-optical parameters rather than by differences in atmospheric structure. On the other hand the differences in the continuum energy distributions in Figs 2–5 clearly apparent in the UV are caused primarily by changes in the atmospheric structure.

To determine the effects of altered line blanketing due to the presence of the magnetic field on the spectra of magnetic white dwarfs, we proceeded as follows. The ATLAS line-blanketed atmosphere with magnetic field was calculated – as shown in Figs 2–5 – and the continuum opacity and related parameters such as hydrogen number density were extracted. Then these data were fed in as input to our standard program for producing the spectrum from a magnetic white dwarf. The latter program uses an atmospheric structure as an input and adds in hydrogen line opacities appropriately shifted according to the magnetic field at different parts of the stellar surface (Wickramasinghe & Martin 1979). The continuum opacity is also shifted according to the formula of Lamb & Sutherland (1974).

The net output depends on several effects of the magnetic field, of which the two most important are:

(i) altered line blanketing from the field;

(ii) magnetic broadening due to different field strengths across the surface of the star.

In this paper we are concerned with the significance of the first effect. In order to separate out its effect, we use the artificial procedure of putting *different* line-blanketed atmospheres (the temperature and pressure structure) into the magnetic broadening program with the *same* linewidths. The thing which we set out to test was whether the effect of the magnetic field on the atmospheric structure leads to any effect on the spectrum of a magnetic white dwarf. Accordingly, we generated a series of pairs of models. The first model in each pair used a zero-field atmospheric structure (the one shown in Fig. 1) and the second model in each pair used a 50 MG atmospheric structure, namely one of the models shown in Figs 2–5. These pairs of structures were then plugged into an identical magnetic-broadening program, namely the program set up with the same linewidth parameters as the 50 MG atmospheric structure. Sample pairs of models are described in Tables 4 and 5.

Table 4. Assumptions behind the pair of models compared in Figs 6 & 7.

	First model	Second model
Continuum opacity	ATLAS line-blanketed atmosphere, $B=0$.	ATLAS line-blanketed atmosphere, constant $B=50\,MG$, constant viewing angle $i=45°$, linewidths unchanged
Line opacity	Pressure-broadened lines	Pressure-broadened lines
Calculation	Continuum and line opacities shifted in the presence of a dipole magnetic field of polar strength $50\,MG$, viewing angle $i=0°$	Continuum and line opacities shifted in the presence of a dipole magnetic field of polar strength $50\,MG$, viewing angle $i=0°$

Table 5. Assumptions behind the pair of models compared in Figs 8 & 9.

	First model	Second model
Continuum opacity	ATLAS line-blanketed atmosphere, $B=0$.	ATLAS atmosphere, constant $B=50\,MG$, viewing angle $i=45°$, no lines
Line opacity	Doppler-broadened lines	Doppler-broadened lines
Calculation	Continuum and line opacities shifted in the presence of a dipole magnetic field of polar strength $50\,MG$, viewing angle $i=0°$	Continuum and line opacities shifted in the presence of a dipole magnetic field of polar strength $50\,MG$, viewing angle $i=0°$

There are two differences between the ATLAS modelling process and the magnetic-broadening program which should be remarked upon. First, in the ATLAS model we used a constant field of $50\,MG$ while in the magnetic-broadening program the dipole strength is $50\,MG$, which means that the field ranges from $50\,MG$ at the pole to $25\,MG$ at the equator. We used only a single field for the ATLAS modelling because generating a range of ATLAS models would require an exorbitant amount of computing effort, to little effect (considering the results). Therefore the differences between the first and second models in each pair are somewhat exaggerated.

Second, the ATLAS atmosphere uses a constant viewing angle $i=45°$ whereas the magnetic-broadening program uses the viewing angle $i=0°$. But since the magnetic-broadening program averages the solution over the surface of the star, the angle between the normal to the surface and the viewing direction ranges from $0°$ to $90°$. Therefore the value $i=45°$ used in the ATLAS program is a reasonable compromise.

The results are shown in Figs 6–9. The finding in Fig. 6 is dramatic: when no reduction in line component widths is assumed in the presence of a magnetic field, the effect of different degrees of line blanketing on the line spectrum is negligible. The main difference is that there is some change in the total flux. (This is possible since only the continuum opacities and atmospheric structures corresponding to Figs 1 & 2 were used in calculating Fig. 6, the line opacities being treated differently.) The appearance of the Balmer absorption lines is almost identical. The reason for this is that the magnetic broadening spreads the line opacities across many different wavelengths, and hence the line opacities dominate over the continuum opacities in the optical region.

Fig. 7 shows the circular polarization corresponding to the fluxes in Fig. 6. There are only marginal differences between the polarizations in the two models. One striking result is very large polarization values – approaching 1 or -1 – near the Lyman lines. These large values are found in
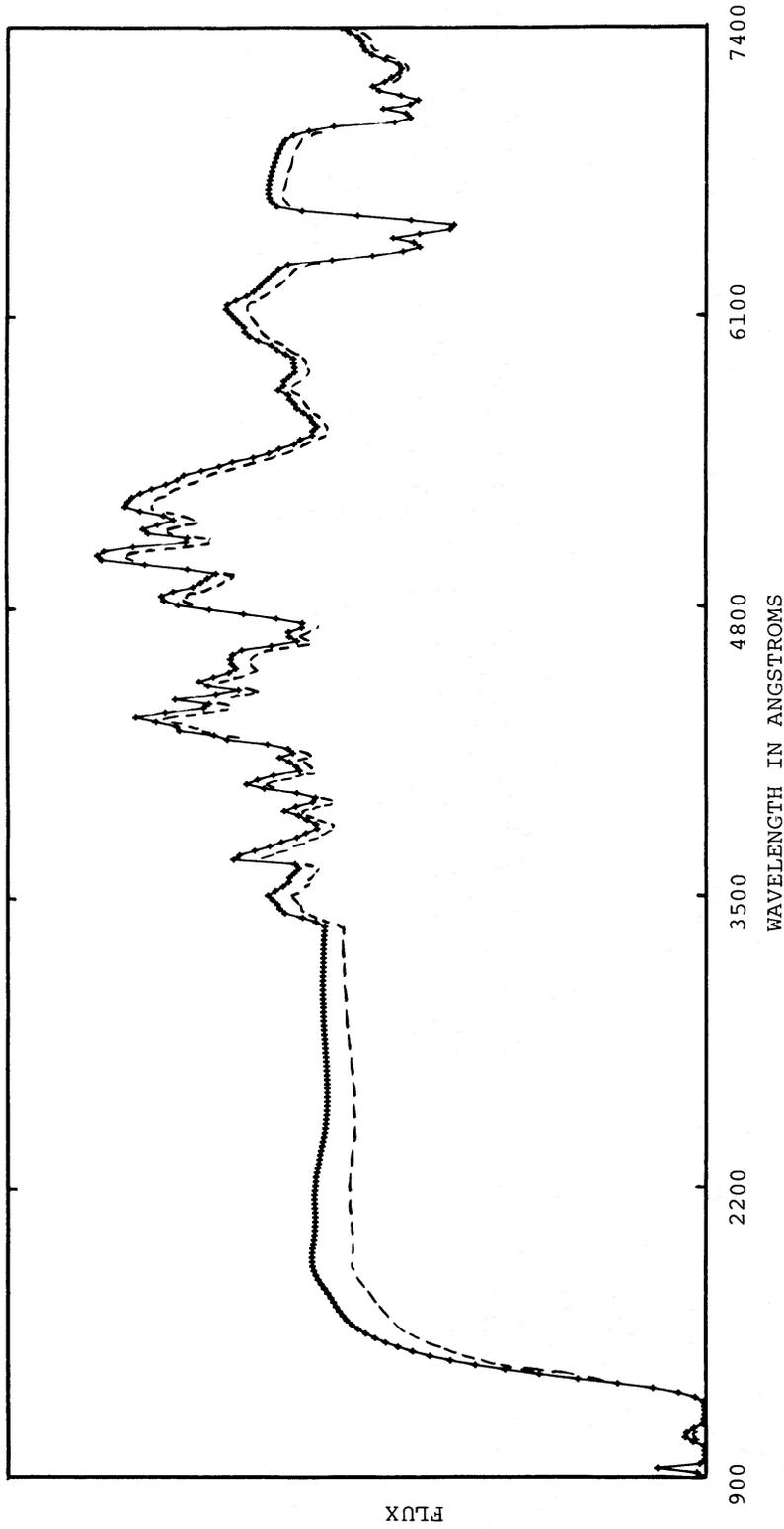
Figure 6. Fluxes F_ν from a pure hydrogen white dwarf atmosphere with $T_e = 12\,000$ K and gravity $\log g = 8.0$ in the presence of a centred dipole magnetic field of polar strength $B = 50$ MG, viewed from the pole. For the solid (top) curve the atmospheric structure and the unshifted continuum opacity is taken from the $B = 50$ MG atmosphere shown in Fig. 2. For the dashed (bottom) curve the atmospheric structure and the unshifted continuum opacity is taken from the $B = 0$ atmosphere shown in Fig. 1. The linewidth factors are the same for both curves. See Table 4. At the top of the graph $F_\nu = 0.0012$ erg cm^{-2} s^{-1} Hz^{-1}.
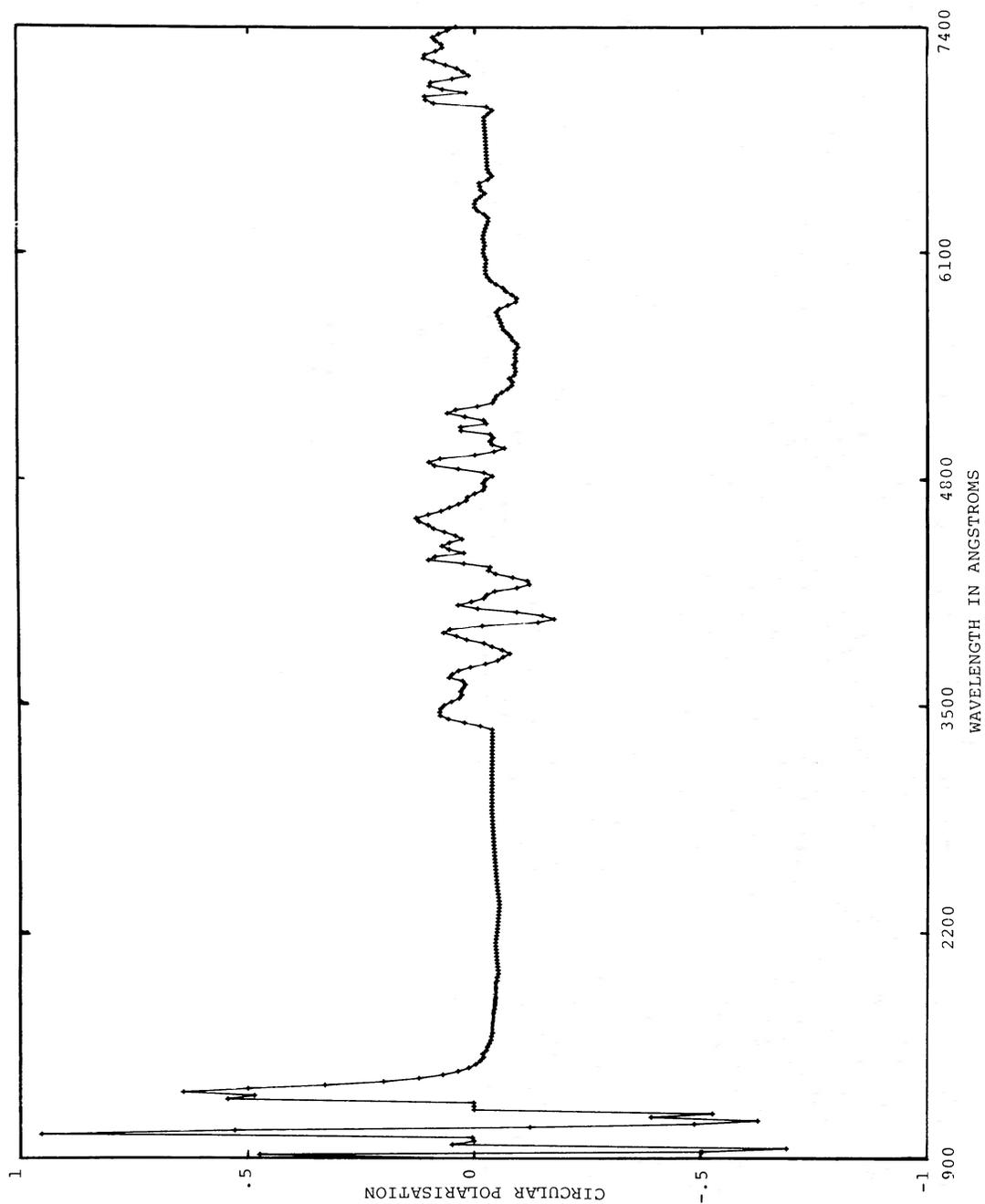
Figure 7. Circular polarization corresponding to the fluxes in Fig. 6. The differences in the curves are too small to be shown.

Figure 8. Fluxes F_ν from a pure hydrogen white dwarf atmosphere with $T_e = 12\,000$ K and gravity log $g = 8.0$ in the presence of a centred dipole magnetic field of polar strength $B = 50$MG, viewed from the pole. For the solid (bottom) curve the atmospheric structure and the unshifted continuum opacity is taken from the $B = 50$MG atmosphere shown in Fig. 4. For the dashed (top) curve the atmospheric structure and the unshifted continuum opacity is taken from the $B = 0$ atmosphere shown in Fig. 1. The linewidth factors are the same for both curves. See Table 5. At the top of the graph $F_\nu = 0.0012$ erg cm^{-1} s^{-1} Hz^{-1}.
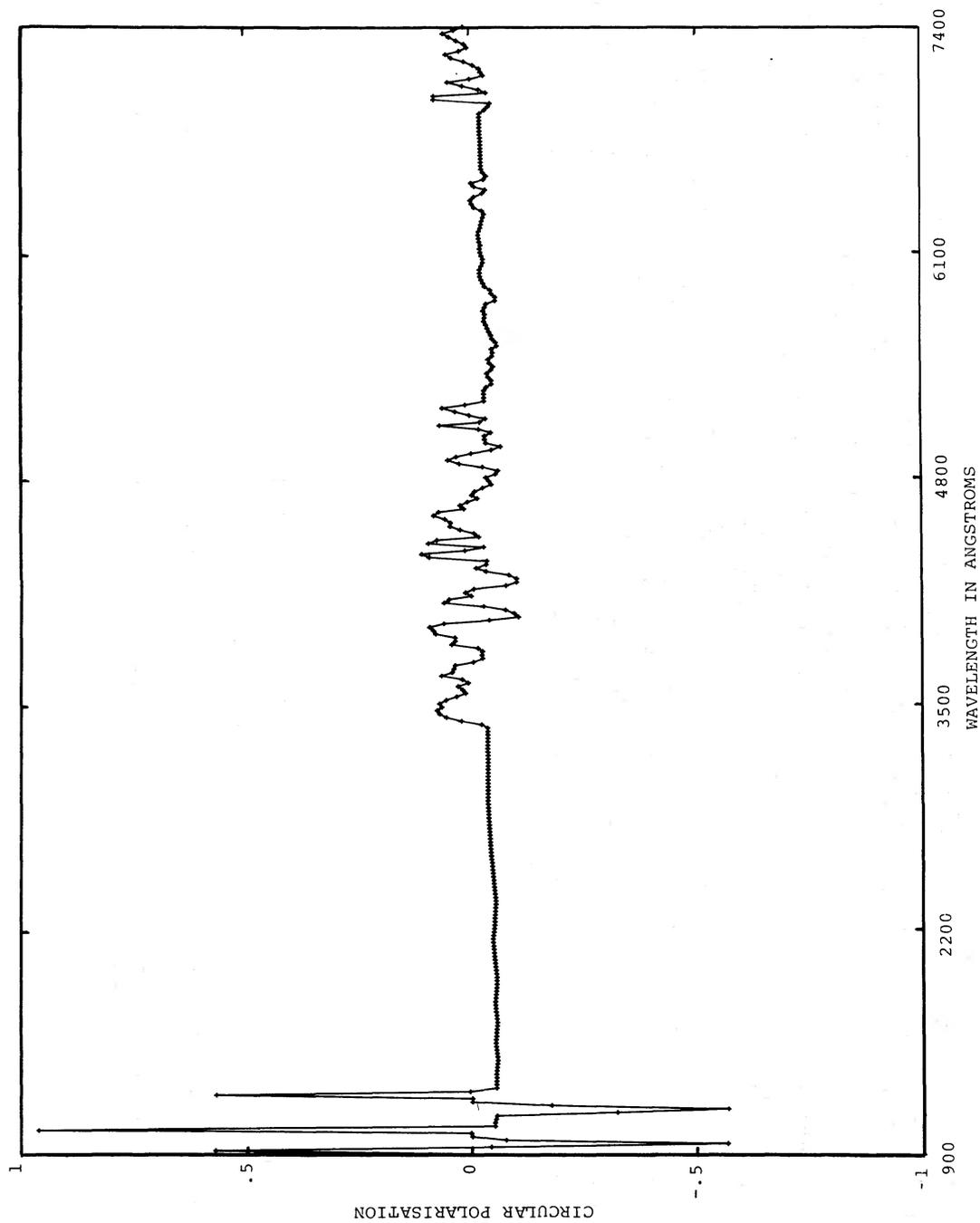
Figure 9. Circular polarization corresponding to the fluxes in Fig. 8. The differences in the curves are too small to be shown.

the wings of Lyman α and β. The wavelength dependence of polarization in this region is characteristic of Zeeman triplet splitting of Lyα and β. There is also a large value of polarization near the Lyman jump similar to that found near the Balmer jump. These jumps in polarization are due to the continuum shifts.

Figs 8 & 9 give similar results for the case of Doppler broadening only. The differences in flux shown in Fig. 8 are much more than in Fig. 6, as expected due to the larger redistribution of flux in Fig. 4. Nevertheless, the basic appearance of the absorption lines in the optical region is much the same. The most important difference is in the continuum slope blueward of the Balmer jump. There are slightly greater differences in the circular polarization in Fig. 9.

Our basic conclusion is simple: the inclusion of magnetic line blanketing does not have much effect on the overall appearance of the spectra of magnetic white dwarfs in the optical region, since magnetic broadening due to field spread dominates over effects caused by changes in atmospheric structure. This is a negative result, but quite an unexpected one. It means that the reliance on zero-field atmospheres in previous models of magnetic white dwarfs is likely to be quite satisfactory for analyses of optical spectra.

In reaching our conclusion, we developed a convenient way of calculating an approximation for the intensity in polarized radiative transfer using only a single equation. We also found enormous polarizations near the Lyman lines and jump. Our project also points to the need to determine linewidths in the presence of a magnetic field: the uncertainty in this factor outweighs all other assumptions made in our calculations.

References

Allen, C. W., 1976. *Astrophysical Quantities*, Athlone Press, London.
Angel, J. R. P., 1978. *Ann. Rev. Astr. Astrophys.*, **16**, 487.
Angel, J. R. P., Borra, E. F. & Landstreet, J. D., 1981. *Astrophys. J. Suppl.*, **45**, 457.
Beckers, J. M., 1969. *Sol. Phys.*, **9**, 372.
Borra, E. F., 1976. *Astrophys. J.*, **209**, 858.
Forster, H., Strupat, W., Rösner, W., Wunner, G., Ruder, H. & Herold, H., 1984. *J. Phys. B: At. Mol. Phys.*, **17**, 1301.
Greenstein, J. L., Henry, R. J. W. & O'Connell, R. F., 1985. *Astrophys. J.*, **289**, L25.
Hardorp, J., Shore, S. N. & Wittmann, A., 1976. *Physics of A_p Stars*, p. 419, eds Weis, W. W., Jekner, H. & Wood, H. J., Universitätssternwarte Wien, Vienna.
Henry, R. J. W. & O'Connell, R. F., 1985. *Publs astr. Soc. Pacif.*, **97**, 333.
Kemic, S. B., 1974. *Jt Inst. Lab. Astr. Rep. 113.*
Kurucz, R., 1971. *Smith. astr. Obs. Spec. Rep. 309.*
Lamb, F. K. & Sutherland, P. G., 1974. *Physics of Dense Mater*, p. 265, ed. Hansen, C. J., Reidel, Dordrecht, Holland.
Landstreet, J. D., 1985. Preprint.
Liebert, J., Angel, J. R. P. & Landstreet, J. D., 1975. *Astrophys. J.*, **202**, L139.
Martin, B. & Wickramasinghe, D. T., 1979. *Mon. Not. R. astr. Soc.*, **189**, 883.
Martin, B. & Wickramasinghe, D. T., 1981. *Mon. Not. R. astr. Soc.*, **196**, 23.
Martin, B. & Wickramasinghe, D. T., 1982. *Mon. Not. R. astr. Soc.*, **200**, 993.
Martin, B. & Wickramasinghe, D. T., 1984. *Mon. Not. R. astr. Soc.*, **206**, 407.
O'Donoghue, D. E., 1980. *Astrophys. Space Sci.*, **68**, 273.
Pacholczyk, A. G., 1976. *Radio Galaxies*, Pergamon Press, London.
Smith, E. R., Henry, R. J. W., Surmelian, G. L. & O'Connell, R. F., 1972. *Astrophys. J.*, **179**, 659.
Stenflo, J. O., 1971. *Solar Magnetic fields*, p. 101, ed. Howard, R., Reidel, Dordrecht, Holland.

Unno, W., 1956. *Publs astr. Soc. Japan*, **8**, 108.
Wickramasinghe, D. T., 1972. *Mem. R. astr. Soc.*, **76**, 129.
Wickramasinghe, D. T. & Martin, B., 1979. *Mon. Not. R. astr. Soc.*, **188**, 165.

Appendix: Oscillator strengths in the presence of a magnetic field

In the modelling of magnetic white dwarfs, it is necessary to know oscillator strengths for individual components of absorption lines, in particular the Lyman and Balmer lines of hydrogen in the presence of a magnetic field. Since there are a number of different tabulations, definitions and formulas in the literature, with some apparent discrepancies, we think it may be useful to spell out what is involved.

If we look at Allen's tabulated values of the weighted oscillator strengths for a particular line (say H_α) we find that the values are smaller by a factor of 3 in comparison with the straight sum of the oscillator strengths of the Zeeman components tabulated by Forster *et al.* (1984) in the limit $B \to 0$. This apparent discrepancy is reflected in the definitions of f_{ij} given by Allen (1976) and Forster *et al.* (1984).

In fact there is no discrepancy since the Forster *et al.* values apply to individual Zeeman components each with a specific polarization ($\Delta m = 0, \pm 1$). The f_{ij} values of individual components should not be added as a straight sum but should be combined as in equation (5) when calculating opacities of blends of Zeeman lines. To clarify this point we look at the radiative-transfer equation for Zeeman components in a Zeeman triplet. We see that the effective opacity at zero-field becomes η_I, which is given by (5). At zero-field, $\eta_p = \eta_l = \eta_r = \eta$, and hence $\eta_I = \eta$ also. However, if one *added up* the oscillator strengths given by Forster *et al.* the result would be three times as large as the values given by Allen.

Kemic (1974) defines the strengths of a transition S_{ij} with an extra factor of $(2S+1)=2$. Indeed, his tabulated S_{ij} values are twice as large as Forster *et al*'s dipole strengths $d_{\tau',\tau}$. But in Kemic's formulas for f_{ji} the $(2S+1)$ factor is divided out, so there is no factor of 2 discrepancy. However Kemic's formula for f_{ji} gives values that are a factor 3 smaller than the values given by Forster *et al.*

Smith *et al.* (1972) give values for the transition probability A_{ij}. Aside from their minor erratum, their formula (3) and their results are smaller by a factor if $8\pi/3$ from the values of Forster *et al.* There is no discrepancy since Smith *et al.*'s definition is for emission into unit solid angle in the forward direction.